Spin Waves and Electronic Interactions in La$_2$CuO$_4$

R. Coldea[1,2], S.M. Hayden[3], G. Aeppli[4], T.G. Perring[2], C.D. Frost[2], T.E. Mason[1], S.-W. Cheong[5], and Z. Fisk[6]

[1] *Oak Ridge National Laboratory, Oak Ridge, TN 37831, USA*
[2] *ISIS Facility, Rutherford Appleton Laboratory, Chilton, Didcot, OX11 0QX, UK*
[3] *H.H. Wills Physics Laboratory, University of Bristol, Bristol, BS8 1TL, UK*
[4] *NEC Research Institute, Princeton, NJ 08540, USA*
[5] *Lucent Technologies, Murray Hill, NJ 07974, USA*
[6] *Department of Physics, Florida State University, Tallahassee, Florida 32306, USA*

(5 April 2001)

The magnetic excitations of the square-lattice spin-1/2 antiferromagnet and high-Tc parent La$_2$CuO$_4$ are determined using high-resolution inelastic neutron scattering. Sharp spin waves with absolute intensities in agreement with theory including quantum corrections are found throughout the Brillouin zone. The observed dispersion relation shows evidence for substantial interactions beyond the nearest-neighbor Heisenberg term, which can be understood in terms of a cyclic or ring exchange due to the strong hybridization path around the Cu$_4$O$_4$ square plaquettes.

While there is consensus about the basic phenomenology - electron pairs with non-zero angular momentum, unconventional metallic behavior in the normal state, tendencies towards inhomogeneous charge and spin density order - of the high temperature copper oxide superconductors, there is no agreement about the microscopic mechanism. After over a decade of intense activity, there is not even consensus as to the simplest "effective Hamiltonian", which is a short-hand description of the motions and interactions of the valence electrons, needed to account for cuprate superconductivity. Because much speculation is centered on magnetic mechanisms for the superconductivity, it is important to identify the interactions among the spins derived from the unfilled Cu^{2+} d-shells. The present experiments show that there are significant (on the scale of the pairing energies for high-Tc superconductivity) interactions coupling spins at distances beyond the 3.8 Å separation of nearest-neighbor Cu^{2+} ions. Cyclic or ring exchange due to a strong hybridization path around the Cu$_4$O$_4$ squares (see Fig. 1A), from which the cuprates are built, provides a natural explanation for the measured dispersion relation. CuO$_2$ planes are thus the second example of an important Fermi system (^{3}He is the other [1]) where significant cyclic exchange terms have been deduced.

Magnetic interactions are revealed through the wavevector dependence or dispersion of the magnetic excitations. In magnetically ordered materials, the dominant excitations are spin waves which are coherent (from site to site as well as in time) precessions of the spins about their mean values. The lower frame of Fig. 1B shows the dispersion relation calculated using conventional linear spin-wave theory in the classical large-S limit, where the only magnetic interaction is a strong nearest-neighbor superexchange coupling J [2]. We identify wavevectors by their coordinates (h, k) in the two-dimensional (2D) reciprocal space of the square lattice.

Spin waves emerge from the wavevector $(1/2,1/2)$ characterizing the simple antiferromagnetic (AF) unit cell doubling in La$_2$CuO$_4$ [3], and disperse to reach a maximum energy $2J$ that is a constant along the AF zone boundary marked by dashed squares in Fig. 1B. Longer-range interactions manifest themselves most simply at the zone boundary. The upper frame of Fig. 1B shows the dispersion calculated with modest interactions between next nearest-neighbors. Virtually the only visible effect of the additional interactions is the dispersion of the spin waves along the zone edge. Thus, experiments to test for such interactions must measure the spin waves along the zone boundary. Only inelastic neutron scattering with high energy and wavevector resolution can accomplish this, although photon spectroscopy [4–7] has led to suspicions of such interactions.

For La$_2$CuO$_4$, a requirement that complicates meeting the resolution goals is the need to use neutrons with energies in the epithermal, 0.1-1.0 eV, range rather than in the more conventional cold and thermal [8], 2-50 meV, regimes. An early high energy neutron scattering experiment [9] revealed well-defined spin-wave excitations throughout the Brillouin zone which could be modeled using a nearest-neighbor Heisenberg exchange J=136 meV. The directions of the scattered neutrons were specified only to within the solid angle determined by the large detector dimensions. Thus, the measured spectra represented averages over large portions of the reciprocal space, so that dispersion along the zone boundary was unresolvable and only an upper bound could be placed on further neighbor couplings. The advance enabling the present investigation is the use of position-sensitive detectors for the scattered neutrons, which increases the wavevector resolution by an order of magnitude. The new detector bank is installed in the direct-geometry High-Energy Transfer (HET) time-of-flight spectrometer at the ISIS proton-driven pulsed neutron spallation source.
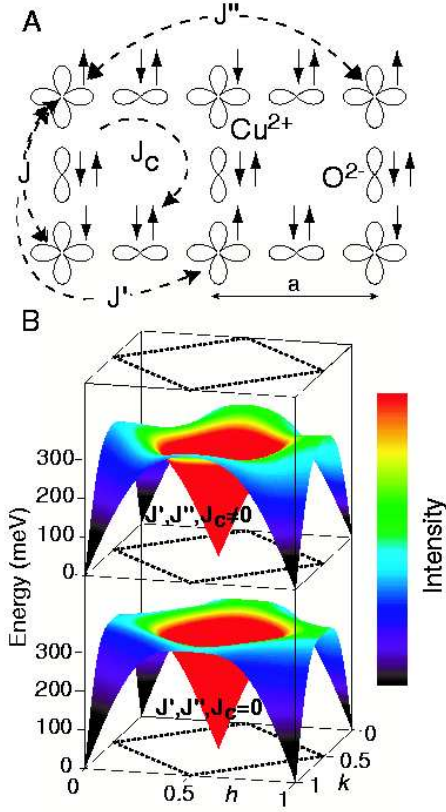
FIG. 1. (color) **A** The CuO$_2$ plane showing the atomic orbitals (Cu $3d_{x^2-y^2}$ and O $2p_{x,y}$) involved in the magnetic interactions. J, J' and J'' are the first-, second- and third-nearest-neighbor exchanges and J_c is the cyclic interaction which couples spins at the corners of a square plaquette. Arrows indicate the spins of the valence electrons involved in the exchange. **B** Lower surface is the dispersion relation for J=136 meV and no higher-order magnetic couplings or quantum corrections. The upper surface shows the effect of the higher-order magnetic interactions determined by the present experiment. Color is spin-wave intensity.

Fig. 2A shows data in the form of constant energy scans for wavevectors around the antiferromagnetic zone center. As E increases, counter-propagating modes become apparent. As the zone boundary is approached and there is less dispersion, inspection of Fig. 1B reveals that it should be easier to locate the spin waves via energy scans performed at fixed wavevector. Fig. 2B shows a series of such scans collected at various points along the zone boundary. The spin waves have a clearly noticeable dispersion, from a minimum of 292±7 meV near $\boldsymbol{Q}$=(3/4,1/4) to a maximum of 314±7 meV near (1/2,0). This is in obvious contrast to the dispersion-less behavior of linear spin-wave theory for the nearest-neighbor Heisenberg model. We have collected data throughout the Brillouin zone and Fig. 3A shows the resulting dispersion along major symmetry directions obtained from cuts of the type shown in Fig. 2. Fig. 3B displays the corresponding spin-wave intensities, in absolute units cali-
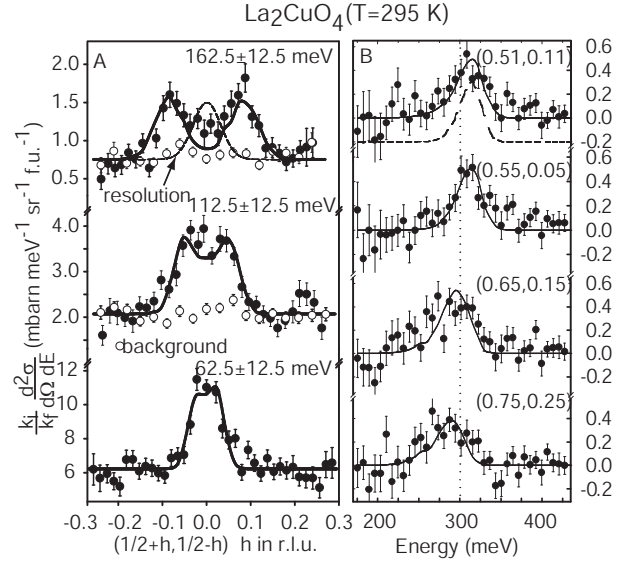

FIG. 2. Scattering from the spin waves in La$_2$CuO$_4$ (T=295 K). Data result from 68 hours (A) and 98 hours (B) counting at a proton current of 170 μA. The sample is described in [10]. Solid lines are fits to a spin-wave cross-section convolved with the instrumental resolution. (A) Const-E cuts near the AF zone center for an incident energy E_i=250 meV. Q_z wavevector components at scan centers are l=2.8 (bottom panel), 6.2 and 9.6 r.l.u. Open circles are a background measured near the (0,0) position. Dashed curve is the instrumental response to spin waves of infinite velocity. (B) Const-Q cuts, with E_i=750 meV, yield the dispersion along the AF zone boundary. Vertical dotted line at E=300 meV is a guide to the eye. l values at peak position vary from 8.8 (bottom panel) to 9.5 (top panel). A background measured near the nuclear zone center (1,0) has been subtracted. Dashed curve is the instrumental response to a dispersionless mode.

brated using acoustic phonon scattering from the sample.

To understand our results, we consider a Heisenberg Hamiltonian including higher order couplings [11–14]

$$\mathcal{H} = J \sum_{\langle i,j \rangle} \boldsymbol{S}_i \cdot \boldsymbol{S}_j + J' \sum_{\langle i,i' \rangle} \boldsymbol{S}_i \cdot \boldsymbol{S}_{i'} + J'' \sum_{\langle i,i'' \rangle} \boldsymbol{S}_i \cdot \boldsymbol{S}_{i''}$$
$$+ J_c \sum_{\langle i,j,k,l \rangle} \{ (\boldsymbol{S}_i \cdot \boldsymbol{S}_j)(\boldsymbol{S}_k \cdot \boldsymbol{S}_l) + (\boldsymbol{S}_i \cdot \boldsymbol{S}_l)(\boldsymbol{S}_k \cdot \boldsymbol{S}_j)$$
$$- (\boldsymbol{S}_i \cdot \boldsymbol{S}_k)(\boldsymbol{S}_j \cdot \boldsymbol{S}_l) \}, \tag{1}$$

where J, J' and J'' are the first-, second- and third-nearest-neighbor magnetic exchanges where the paths are illustrated in Fig. 1A. J_c is the ring exchange interaction coupling four spins (labelled clockwise) at the corners of a square plaquette. Each spin coupling is counted once in Eq. (1). Using classical (large-S) linear spin-wave theory the dispersion relation is [13,15] $\omega_{\boldsymbol{Q}}$=$2Z_c(\boldsymbol{Q})\sqrt{A_{\boldsymbol{Q}}^2 - B_{\boldsymbol{Q}}^2}$, $A_{\boldsymbol{Q}}$=$J - J_c/2 - (J' - J_c/4)(1 - \nu_h\nu_k) - J''[1 - (\nu_{2h} + \nu_{2k})/2]$, $B_{\boldsymbol{Q}}$=$(J - J_c/2)(\nu_h + \nu_k)/2$, $\nu_x = \cos(2\pi x)$ and $Z_c(\boldsymbol{Q})$ is a renormalization factor [16]

2

that includes the effect of quantum fluctuations. Within linear spin-wave theory all three higher-order spin couplings (J', J'' and J_c) have similar effects on the dispersion relation and intensity dependence, therefore they cannot be determined independently from the data without additional constraints. We first assume that only J and J' are significant as in [17], i.e. $J''=J_c=0$. The solid lines in Fig. 2 are fits to a one-magnon cross-section and Fig. 3 shows fits to the extracted dispersion relation and spin-wave intensity. As can be seen in the figures, the model provides an excellent description of both the spin-wave energies and intensities. The extracted nearest-neighbor exchange $J=111.8\pm4$ meV is antiferromagnetic, while the next-nearest-neighbor exchange $J'=-11.4\pm3$ meV across the diagonal is *ferromagnetic*. A wavevector-independent quantum renormalization factor [16] $Z_c=1.18$ was used in converting spin-wave energies into exchange couplings. The zone-boundary dispersion becomes more pronounced upon cooling as shown in Fig. 3A and the dispersion at $T=10$ K can be described by the couplings $J=104.1\pm4$ meV and $J'=-18\pm3$ meV.

A ferromagnetic J' contradicts theoretical predictions [19], which give an antiferromagnetic superexchange J'. Wavevector-dependent quantum corrections [20] to the spin-wave energies can also lead to a dispersion along the zone boundary even if $J'=0$, but with sign opposite to our result. Another problem with a ferromagnetic J' comes from measurements on $Sr_2Cu_3O_4Cl_2$ [21]. This material contains a similar exchange path between Cu^{2+} ions to that corresponding to J' in La_2CuO_4 and analysis of the measured spin-wave dispersion leads to an antiferromagnetic exchange coupling for this path [21].

While we can cannot definitively rule out a ferromagnetic J' we can obtain a natural description of the data in terms of a one-band Hubbard model [22], an expansion of which yields the spin Hamiltonian in Eq. (1) where the higher-order exchange terms arise from the coherent motion of electrons beyond nearest-neighbor sites [11–13]. The Hubbard Hamiltonian has been widely used as a starting point for theories of the cuprates and is given by

$$\mathcal{H} = -t \sum_{\langle i,j\rangle,\sigma=\uparrow,\downarrow} \left(c_{i\sigma}^\dagger c_{j\sigma} + \text{H.c.} \right) + U \sum_i n_{i\uparrow} n_{i\downarrow}, \quad (2)$$

where $\langle i,j \rangle$ stands for pairs of nearest-neighbors counted once. Eq. (2) has two contributions: the first is the kinetic term characterized by a hopping energy t between nearest-neighbor Cu sites and the second the potential energy term with U being the penalty for double occupancy on a given site. At half filling, the case for La_2CuO_4, there is one electron per site and for $t/U \to 0$, charge fluctuations are entirely suppressed in the ground state. The remaining degrees of freedom are the spins of the electrons localized at each site. For small but non-zero t/U, the spins interact via a series of exchange terms, as in Eq.(1), due to coherent electron
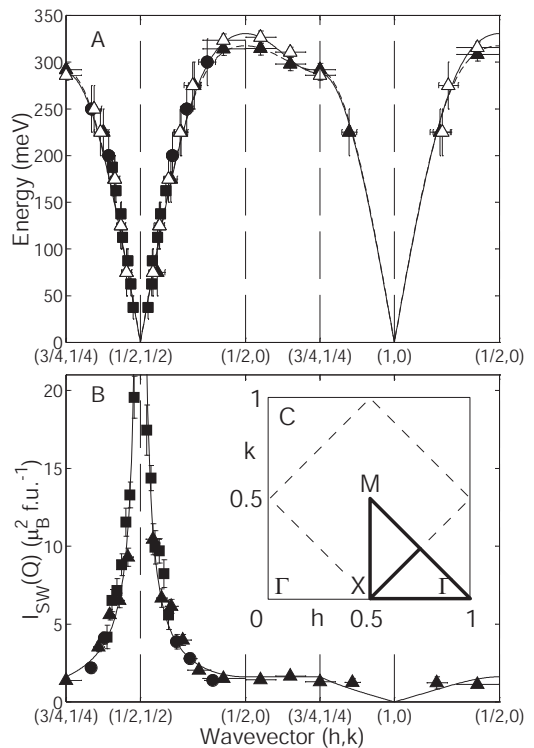

FIG. 3. (A) Dispersion relation along high symmetry directions in the 2D Brillouin zone, see inset (C), at $T=10$ K (open symbols) and 295 K (solid symbols). Squares were obtained for $E_i=250$ meV, circles for $E_i=600$ meV and triangles for $E_i=750$ meV. Points extracted from constant-E(-Q) cuts have a vertical (horizontal) bar to indicate the $E(Q)$ integration band. Solid (dashed) line is a fit to the spin-wave dispersion relation at $T=10$ K (295 K) as discussed in the text. (B) Wavevector-dependence of the spin-wave intensity at $T=295$ K compared with predictions of linear spin-wave theory shown by the solid line. The absolute intensities [18] yield a wavevector-independent intensity-lowering renormalization factor of 0.51 ± 0.13 in agreement with the theoretical prediction of 0.61 [16] that includes the effects of quantum fluctuations.

motion touching progressively larger numbers of sites. If the perturbation series is expanded to order t^4 (i.e. 4 hops) one regains the Hamiltonian (1) with the exchange constants $J = 4t^2/U - 24t^4/U^3$, $J_c = 80t^4/U^3$ and $J' = J'' = 4t^4/U^3$ [11–13]. We again fitted the dispersion and intensities of the spin-wave excitations using these expressions for the exchange constants and linear spin wave theory. The fits are indistinguishable from those for variable J and J'. Again assuming [23] $Z_c=1.18$, we obtained $t=0.33\pm0.02$ eV and $U=2.9\pm0.4$ eV ($T=295$ K), in agreement with t and U determined from photoemission [24] and optical spectroscopy [25]. The corresponding exchange values are $J=138.3\pm4$ meV, $J_c=38\pm8$ meV and $J'=J''=J_c/20=2\pm0.5$ meV (the parameters at $T=10$ K are $t=0.30\pm0.02$ eV, $U=2.2\pm0.4$ eV, $J=146.3\pm4$ meV and $J_c=61\pm8$ meV). Using these values, the higher-order interactions amount to $\sim$11% ($T=295$

K) of the total magnetic energy $2(J\text{-}J_c/4\text{-}J'\text{-}J'')$ required to reverse one spin on a fully-aligned Nèel phase.

Many results on oxides of copper fall into place when cyclic exchange of the size extracted from our experiments is taken into account. First, the relative magnitude of the cyclic exchange J_c/J=0.27±0.06 at T=295 K (0.41±0.07 at T=10 K) is similar to the ratio of 0.30 estimated from numerical simulations [26] on finite clusters taken from the Cu-O square lattice. Second, magnetic Raman scattering [4,5] and infrared absorption experiments [6,7] show an unusual broadening towards higher energies that cannot be accounted for by a simple (quadratic) Heisenberg Hamiltonian, but can be attributed [5,6] to a cyclic term. Finally, in the related compound $Sr_{14}Cu_{24}O_{41}$, which has square plaquettes stacked to form a ladder, the exchange constants corresponding to the nearly-equal-length rungs and legs of the ladder are 130 meV and 72 meV respectively [27] when no cyclic exchange is included. The inclusion of a ring exchange term [28] J_c=34 meV allows the rungs and legs of the ladder to have similar exchange constants of 121 meV.

We have used a new high-wavevector-resolution epithermal-neutron scattering technique to discover that interactions beyond those coupling nearest-neighbor Cu^{2+} ions are needed to account for the magnetism of La_2CuO_4. The observed further neighbor couplings may be explained by a four-spin cyclic interaction, which arises because the large orbital hybridization in the CuO_2 planes provides an exchange path to include all four spins at the corners of elementary Cu_4O_4 plaquettes. Thus, La_2CuO_4 joins the nuclear magnet ^3He [1] as a system where there is good evidence for substantial ring exchange. Ring exchange occurs even for very simple models, such as the single band Hubbard model, which contains only hopping (t) and on-site Coulomb (U) terms. We have determined t and U using only knowledge - in the form of our spin wave dispersion relation - of charge-neutral excitations and find values in excellent agreement with those obtained via charge-sensitive spectroscopies as well as numerical work on finite clusters. Thus, our results demonstrate that a one-band Hubbard model is an excellent starting point [29] for describing the magnetic interactions in the cuprates, and that even when considering relatively low energy spin excitations, charge fluctuations involving double occupancy must be taken into account. In addition, the scale of the cyclic exchange interactions, which are comparable to pairing energies in the high-Tc materials, implies that they themselves or related electronic currents [30] might be important for superconductivity in the doped cuprates.

[1] M. Roger, J.H. Hetherington, and J.M. Delrieu, Rev. Mod. Phys. **55**, 1 (1983).
[2] P.W. Anderson in *Magnetism*, eds. G.T. Rado and H. Suhl (Academic, New York, 1963), Vol. **1**, p 25.
[3] D. Vaknin *et al.*, Phys. Rev. Lett. **58**, 2802 (1987).
[4] K.B. Lyons *et al.*, Phys. Rev. B **39**, 9693 (1989).
[5] S. Sugai *et al.*, Phys. Rev. B **42**, 1045 (1990).
[6] J. Lorenzana, J. Eroles, and S. Sorella, Phys. Rev. Lett. **83**, 5122 (1999).
[7] J.D. Perkins *et al.*, Phys. Rev. Lett. **71**, 1621 (1993).
[8] G. Shirane *et al.*, Phys. Rev. Lett. **59**, 1613 (1987).
[9] S.M. Hayden *et al.*, Phys. Rev. Lett. **67**, 3622 (1991).
[10] The sample was an array of 7 mutually-aligned single crystals with total mass 48.6 g. Crystals were annealed in argon atmosphere at $800°C$ for 2 hours to achieve the correct oxygen stoichiometry. The Nèel temperature, measured via elastic neutron scattering, was 325±5 K, consistent with the highest values in the literature, see B. Keimer *et al.*, Phys. Rev. B **46**, 14034 (1992).
[11] M. Takahashi, J. Phys. C :Solid State Phys. **10**, 1289 (1977).
[12] M. Roger and J.M. Delrieu, Phys. Rev. B **39**, 2299 (1989).
[13] A.H. MacDonald, S.M. Girvin, and D. Yoshioka, Phys. Rev. B **41**, 2565 (1990); **37**, 9753 (1988).
[14] Anisotropic couplings of less than $10^{-2}J$ are neglected, see C.J. Peters *et al.*, Phys. Rev. B **37**, 9761 (1988).
[15] A. Chubukov, E. Gagliano, and C. Balseiro, Phys. Rev. B **45**, 7889 (1992).
[16] R.R.P. Singh, Phys. Rev. B **39**, 9760 (1989).
[17] R. Coldea *et al.*, Physica B **276-278**, 592 (2000). Data reported in this early paper is the average of the measurements at T=10 K and 295 K.
[18] In extracting spin-wave intensities we used the Cu^{2+} $3d_{x^2-y^2}$ magnetic form factor and assumed a spherical distribution of ordered Nèel domains as in [9].
[19] J.F. Annett *et al.*, Phys. Rev. B **40**, 2620 (1989).
[20] C.M. Canali, S.M. Girvin, and M. Wallin, Phys. Rev. B **45**, 10131 (1992); R.R.P. Singh and M.P. Gelfand, *ibid.* **52**, 15695 (1995); O.F. Syljuåsen and H.M. Rønnow, J. Phys.: Condens. Matter **12**, L405 (2000); H.M. Rønnow *et al.*, cond-mat/0101238.
[21] Y.J. Kim *et al.*, Phys. Rev. Lett. **83**, 852 (1999).
[22] J. Hubbard, Proc. R. Soc. London A **276**, 238 (1963).
[23] Using a wavevector-dependent $Z_c(Q)$ [20] is expected to modify slightly the extracted values of all exchange parameters leading to a larger J_c. Accurate determinations require extending the calculation of $Z_c(Q)$ for the nearest-neighbor model [20] to the case of finite higher-order terms as in Eq. (1).
[24] C. Kim *et al.*, Phys. Rev. Lett. **80**, 4245 (1998).
[25] H.-B. Schüttler and A.J. Fedro, Phys. Rev. B **45**, 7588 (1992).
[26] H.J. Schmidt and Y. Kuramoto, Physica C **167**, 263 (1990); Y. Mizuno, T. Tohyama, and S. Maekawa, J. Low. Temp. Phys. **117**, 389 (1999).

[27] R.S. Eccleston *et al.*, Phys. Rev. Lett. **81**, 1702 (1998).

[28] S. Brehmer *et al.*, Phys. Rev. B **60**, 329 (1999).

[29] P.W. Anderson, Science **235**, 1196 (1987).

[30] T.C. Hsu, J.B. Marston, and I. Affleck, Phys. Rev. B **43**, 2866 (1991); C.M. Varma, *ibid.* **55**, 14554 (1997).